

Electromagnetically Induced Transparency Spectroscopy.

Asaf Eliam¹, Evgeny A. Shapiro¹, Moshe Shapiro^{1,2},

Departments of Chemistry¹ and Physics², The University of British Columbia

2036 Main Mall, Vancouver, BC, Canada V6T 1Z1

(Dated: June 7, 2021)

Abstract

We propose a method based on the Electromagnetically Induced Transparency (EIT) phenomenon for the detection of molecules which exist as a small minority in the presence of a majority of absorbers. The EIT effect we employ effectively eliminates the absorption of the majority species in the spectral region where it overlaps with the absorption of the minority species. The method can also be used to enhance local-modes transitions which overlap spectrally with a background of other local-modes transitions of the same molecule. The general theory is applied to the case of sparse and congested background spectra within the same molecule and to the recording of the spectra of isotopomers (of Chlorine and Methanol) that are in minority relative to other isotopomers which constitute the majority of molecules present.

PACS numbers:

1. INTRODUCTION

Electromagnetically Induced Transparency (EIT)[1–4] is usually observed in three-level atomic systems interacting with two (“probe” and “control”) laser fields. The probe’s electric field, denoted, as illustrated in Fig. 1, by ϵ_1 , is in resonance with the transition frequency between the ground state $|g\rangle$ and an excited state $|e\rangle$. The “control” laser, whose electric field is denoted as ϵ_2 , couples the excited state $|e\rangle$ to an auxiliary state $|s\rangle$. When the conditions are right, quantum interference stabilizes the ground state population, causing the transition from the ground state $|g\rangle$ to the excited state $|e\rangle$ to disappear, rendering the medium *transparent* to the probe field.

An important element at the heart of the EIT effect is that the excited state $|e\rangle$ is coupled to a (radiative or non-radiative) continuum, forming a (scattering) resonance. As depicted schematically in Fig. 1, when such a scattering resonance is dressed radiatively by the control field, it splits into two (Autler-Townes) components[5], forming two overlapping scattering resonances[1, 6–8] which interfere destructively at the position of the bare state energy[6, 9].

This interference results in the appearance of a “dark resonance”[6] or a “dark state”[10, 11] (DS), leading to “Coherent Population Trapping” (CPT)[10, 11] and transparency.

In the general framework of nonlinear optics[12–14], EIT is used in the slowing down[1, 15, 16] and storage[17–21] of light, in quantum teleportation and communication[22], in high precision magnetometry[23], and in developing frequency standards[24]. Related interference phenomena are Electromagnetically Induced Absorption(EIA)[25, 26] and “Laser Induced Continuum Structures” (LICS) [27–30].

The EIT effect is almost insensitive to spontaneous emission from the excited intermediate state, since the population is trapped in the two ground states. Moreover, the transparency window in the absorption spectrum can be controlled via the control of the Autler-Townes(AT)[5] splitting on top of the destructive interference of the two overlapping resonances. These characteristics make EIT a promising tool for high resolution spectroscopy. Indeed, EIT has been used in the spectroscopic studies [15, 25, 31] of alkali atoms, mainly for reducing the inhomogeneous line-widths of absorption lines.

In the present paper we develop EIT as a tool for distinguishing between overlapping transition lines in atomic and molecular systems. An overlap of two or more transition lines in a mixture of different molecules (the “intermolecular” overlap), or in two (local or collective)

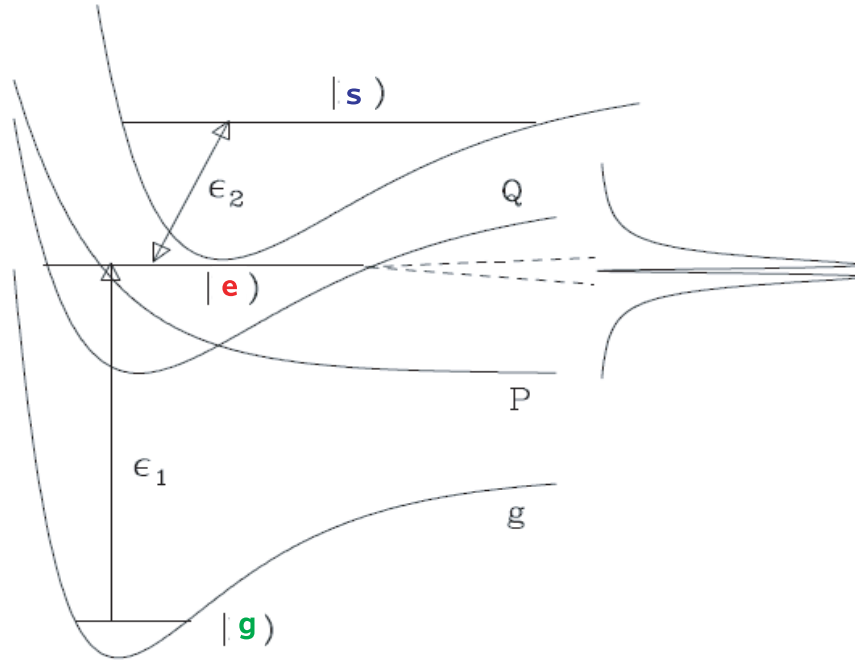


FIG. 1: Molecular EIT: an initial state $|g\rangle$, residing in the ground electronic potential is excited by a weak laser pulse ϵ_1 to a resonance state $|e\rangle$ in electronic state Q , which decays radiatively or non-radiatively to the continuum manifold of electronic state P . The $|e\rangle$ state is coupled optically to a third state $|s\rangle$ by a strong control field ϵ_2 and undergoes as a result Autler-Townes splitting. As a result of the splitting and the decay, an EIT “hole” in the absorption of the probe field ϵ_1 is formed at $E = E_e$.

modes of the same molecule (the “intramolecular” overlap) is a common occurrence[32–35]. Such an overlap can reduce our ability to detect molecules in small concentrations in the presence of molecules in higher concentrations, reduce the accuracy of line assignments, and lead to errors in the derived molecular structure. Line overlaps can also generate a “chain” of misassignments[35], in which errors in the assignments of some lines can lead to the misinterpretation of a whole series, even when it composed of well separated lines.

Commonly used solutions of this problem utilize numerical fitting algorithms. However, numerically distinguishing between spectral lines is not possible when the lines overlap too closely. Likewise, numerical fittings become ineffective when one probes a mixture of different molecules with spectral transitions at similar frequencies. An illustration is given in Fig. 2.

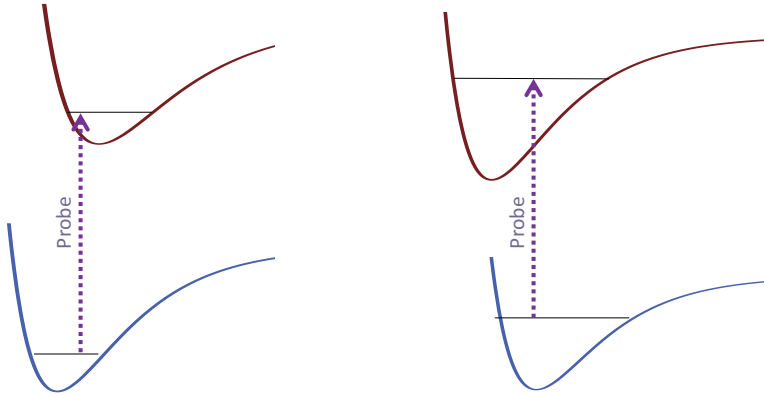


FIG. 2: (Color online) Two overlapping absorption lines related to two different vibronic transitions in two molecules.

The present proposal uses EIT to overcome the overlap problem in both the intramolecular and intermolecular regimes. This is done by applying a “control” field which couples the strongly absorbing states which mask the weakly absorbing lines to some auxiliary states that do not exist (or are out of resonance) in the weakly absorbing species. By making the strongly absorbing lines transparent, the EIT effect helps accentuate the weakly absorbing features, which now stand out against a zero background. In this way, only the desired spectral lines that have not been made transparent remain in the spectrum. The details of the scheme, outlined in Fig.2, are discussed in the next Section.

The structure of this paper is as follows: In section 2 we describe the theory of EIT spectroscopy. In section 3 we discuss the range of applicability of the method and in section 4 we demonstrate the viability of the method by deciphering the spectra in a number of cases where spectral overlaps occur, such as a mixture of Cl_2 isotopomers and in the spectrum of the CH_3OH molecule. In section 5 we discuss the merits of the method and compare it to methods derived from Coherent Anti-Stokes Raman Spectroscopy (CARS) for achieving the same goals.

2. THEORY AND THREE SCENARIOS

2.1. EIT line shapes

We begin by outlining the theory of EIT for strongly decaying intermediate levels [9, 36]. The consideration proceeds in three steps. First, one accounts for the states $|s\rangle$ and $|e\rangle$ in

the three-level configuration depicted in Fig. 1. These states are coupled by the control field characterized by center frequency ω_c , amplitude ϵ_c , and Rabi frequency $\Omega_c = \mu_{e,s}\epsilon_c$. Here $\mu_{e,s}$ are the transition-dipole matrix elements between the $|e\rangle$ and $|s\rangle$ molecular states.

Expressed in the appropriate co-rotating frame, the Hamiltonian within the Rotating Wave approximation is given in atomic units ($\hbar = 1$), as,

$$H_{e,s} = \delta/2 |s\rangle \langle s| - \delta/2 |e\rangle \langle e| + \Omega_c |e\rangle \langle s| + \Omega_c^* |s\rangle \langle e| \quad (1)$$

where $\delta = \omega_c - (E_e - E_s)$ is the detuning of the control field from resonance, E_e and E_s are the bare-states energies. The eigenvalues of this system, given as,

$$l_j = (3 - 2j)\Omega' = (3 - 2j)\sqrt{\delta^2/4 + |\Omega_c|^2}, \quad j = 1, 2, \quad (2)$$

reveal AT split[5] spectra. In the original Schroedinger frame, the corresponding eigenstates are given as[9],

$$|\lambda_j(t)\rangle = \left(\alpha_j |s\rangle e^{i(E_e - E_s + \delta)t} + \beta_j |e\rangle \right) e^{-i(\lambda_j + \delta/2 + E_e)t}, \quad j = 1, 2, \quad (3)$$

where

$$\alpha_j = \left(\frac{|\Omega|^2}{2\Omega'^2 - (3 - 2j)\delta\Omega'} \right)^{1/2}, \quad \text{and} \\ \beta_j = \left(\frac{|\Omega|^2}{2\Omega'^2 - (3 - 2j)\delta\Omega'} \right)^{1/2} \frac{\Omega' - (3 - 2j)\delta/2}{\Omega^*}, \quad j = 1, 2. \quad (4)$$

In the second stage of the development we switch on H_{b-c} , the bound-continuum interaction between state $|e\rangle$ and a continuum of incoming scattering states, $|E, n_1^-\rangle$, where E is the energy and n_1 - the ‘‘channel index’’ - stands for the collection of all the discrete quantum numbers necessary to fully characterize the continuum. The n_1 subscript is a reminder that the $|E, n_1^-\rangle$ states diagonalize only part of the Hamiltonian, the part which does not contain state $|e\rangle$.

In the absence of a control field and when the coupling to the continuum is relatively independent of E , state $|e\rangle$ decays at a rate given by $\Gamma = \pi|V_{e,E}|^2$ [36] where $V_{e,E} \equiv \langle e|H_{b-c}|E, n_1^-\rangle$. The bound-continuum coupling turns each dressed state $|\lambda_{1,2}\rangle$ into a fully interacting scattering resonance $|E, n^-\rangle$, possessing both a bound ($|\lambda_{1,2}\rangle$) component and a continuum ($|E, n_1^-\rangle$) component. Explicit expressions for these eigenstates, found by

applying overlapping resonances Feshbach's or Fano's partitioning techniques[6, 7], can be found in Refs.[9, 36].

At the third stage, we add a ‘‘probe’’ laser, whose electric field is denoted as ϵ_{pr} , to this system. The latter couples the ground state $|g\rangle$ to the continuum of eigenstates $|E, n^-\rangle$. The one-photon absorption probability for a weak probe is given in first order perturbation theory as

$$P_{pr}(E) = 2\pi |\epsilon_{pr}(\omega_E)\mu_{E,g}|^2, \quad (5)$$

where E , the scattering energy, satisfies the resonance condition,

$$E = E_g + \hbar\omega_E, \quad (6)$$

with ω_E being the probe center-frequency. $\mu_{E,g}$ are the transition-dipole matrix elements,

$$\mu_{E,g} = \langle E, n^- | \mu | g \rangle = \sum_{j=1,2} \langle E, n^- | \lambda_j \rangle \langle \lambda_j | \mu | g \rangle. \quad (7)$$

The $\langle E, n^- | \lambda_i \rangle$ overlap integral can be calculated[9] as,

$$\langle E, n^- | \lambda_i \rangle = \sum_j \langle E, n_1^- | H_{b-c} | \lambda_j \rangle \langle \lambda_j | \mathbf{H}(E)^{-1} | \lambda_i \rangle, \quad (8)$$

where $\mathbf{H}(E)$ is an *effective coupling Hamiltonian* describing the continuum-mediated interaction between the field-dressed eigenstates. In the case of an ‘‘unstructured’’ continuum, where $\langle \lambda_j | H_{b-c} | E, n_1^- \rangle = \sqrt{\Gamma/\pi}$, $\mathbf{H}(E)$ can be expressed as

$$\mathbf{H}(E) = \begin{pmatrix} E - E_e - \delta/2 - \lambda_1 - i\Gamma/2 & -i\Gamma/2 \\ -i\Gamma/2 & E - E_e - \delta/2 - \lambda_2 - i\Gamma/2 \end{pmatrix}. \quad (9)$$

The diagonal matrix elements of Eq. (9) embody the AT level splitting, and the off-diagonal elements describe the coupling to the continuum.

Equations (8,9) lead to the final expression

$$\mu_{E,g} = V_{E,e} \left\{ |\alpha_1|^2 D_{11} + \alpha_1 \alpha_2^* D_{12} + \alpha_2 \alpha_1^* D_{21} + |\alpha_2|^2 D_{22} \right\}, \quad (10)$$

where $D_{ij} = \mathbf{H}_{i,j}^{-1}$, and α_j is given by Eq.(4). If the control detuning $\delta = 0$, then

$$\mu_{E,g} = \frac{1}{D} \mu_{e,s} V_{E,e} [E - E_e], \quad (11)$$

where

$$D = [E - E_g - i\Gamma/4]^2 + \Gamma^2/16 - \Omega_c^2. \quad (12)$$

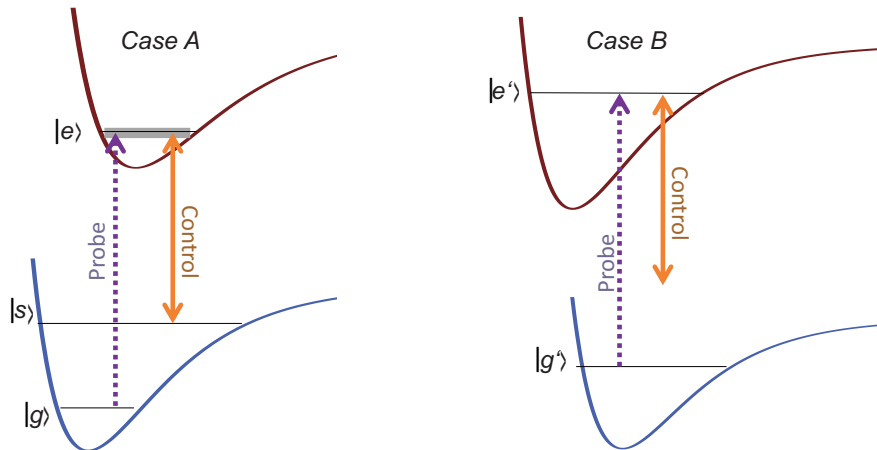


FIG. 3: (Color online) EIT assisted spectroscopic probing. A strong control field eliminates one of the overlapping lines from the absorption spectrum. This field is not in resonance with any strong transition in the second molecule.

Expressions (5,10,11) will be used below for calculating the field-modified absorption spectra of molecules.

2.2. Intermolecular EIT spectroscopy

As a first application we consider the use of EIT in resolving spectral overlaps in the “intermolecular” case, shown in Figure 2, in which one molecule in a mixture overshadows the absorption of another. Here EIT spectroscopy amounts to the application of a control field which is in resonance with a transition belonging to just one of the molecules/atoms in the mixture, thereby making that molecule transparent at the probe’s frequency, bringing out the absorption lines of other molecules. Such a configuration is shown in Figure 3.

Denoting the absorption lines we wish to eliminate from the spectrum as “*A* lines”, and the ones we want to preserve – “*B* lines”, the scheme will succeed if the control field eliminating the *A* lines will not modify the *B* lines in any substantial way. This condition is fulfilled, as discussed in greater detail below, if the control field is far from resonance for all the *B* lines.

A simple illustration of the intermolecular scenario is given in Figure (4). Panel (a)

shows two overlapping spectral lines of Lorentzian profile, of the same height and same width Γ , whose center-line positions are separated by $\Gamma/4$. This small separation relative to the widths does not allow resolving by ordinary means one line in preference to the other. In Panel (b) we show the result of a calculation performed according to Eqs. (5,11) with $\Omega_c = 2.5\Gamma$, verifying that a resonant control field effectively eliminates one of the A lines, leaving, due to its being off-resonance with the control laser field, the B line unaffected. In order to estimate the required control intensity, we take a typical value of $\Gamma = 0.01 \text{ cm}^{-1}$. This translates into $\Omega_c = 0.75 \text{ GHz}$. For $\mu_{s,e} = 0.1 \text{ Debye}$, the required control field intensity is merely $I_c = 15 \text{ kW/cm}^2$.

2.3. Intramolecular EIT spectroscopy: Elimination of many overlapping transitions in the same molecule

In a similar fashion we can eliminate one transition which overlaps with another within the same molecule. This case may however be more complicated due to the fact that in a thermal initial ensemble the spectrum may contain many $|g\rangle$ to $|e\rangle$ transitions which strongly overlap. Moreover, in large molecules, even if thermally cooled, the B line can be embedded in a congested spectrum of close-lying transitions. For the method to succeed, one needs to ensure that *all* the neighboring A lines are made transparent or are pushed away, not just those which are in exact resonance with the control field, leaving no trace in the spectral region of interest. The method will fail if some of the neighboring A lines are pushed into the region of interest rather than away from it.

The case of many A absorption lines is investigated in Fig.5. Panel (a) shows a spectrum comprised of five lines of the same Γ widths, whose line positions are separated by 2Γ . The task is to eliminate all the spectral features from the region surrounding $\omega = \omega_{res}$. Panels (b)-(d) show the effect of a control field, in resonance with the central line, on all the lines in the spectrum. The control Rabi frequency is set as $\Omega = 2\Gamma, 4\Gamma$, and 6Γ respectively. The change in the spectrum due to the control field, which is now off-resonant for most of the lines, is calculated for each line according to the formulas (5,10).

Figure 5 clearly shows that the control pulse can indeed part the congested A spectrum, removing A lines that are both on- and off-resonance with the control field. The pulse intensities remain essentially the same as in the case of just two overlapping lines.

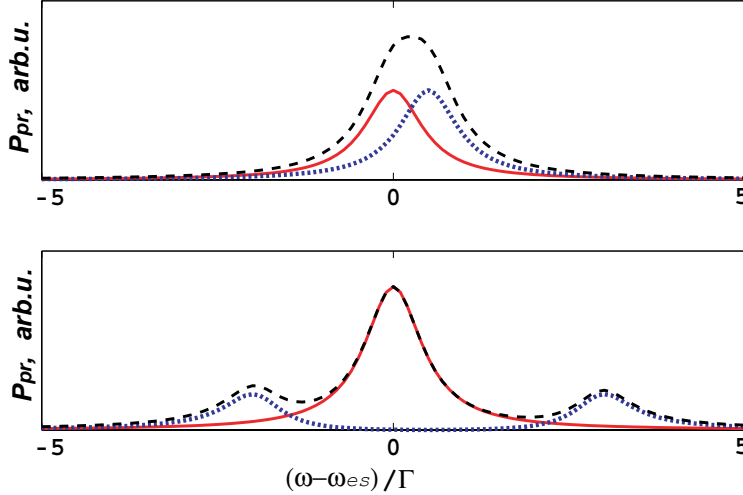


FIG. 4: (Color online) Use of EIT spectroscopy to resolve two overlapping lines. The two overlapping absorption lines are shown as dotted blue and solid red lines. Their joint envelope is shown by the dashed black line. In the upper panel, the spectrum is unperturbed. In the lower panel, one of the absorption lines has been AT-split and removed from the spectrum.

3. CRITERIA OF APPLICABILITY

The condition for the proposed method to work well is for the control field to nullify or push away the A lines absorption while leaving the B lines absorption intact. One can determine whether the B lines are going to be distorted by calculating the energies of the eigenstates modified due to the interaction with the control field. The new frequencies arising in the B spectrum due to AT splitting can be found via an *approximate formula* (2)

$$E_{AT} = E_{e'} + \left[\frac{\delta'}{2} \pm \left(\frac{\delta'}{2} + \frac{2|\Omega'_c|^2}{\delta'} \right) \right]. \quad (13)$$

Here E_{AT} are the (dressed) energies of the AT doublets, $E_{e'}$ is the unperturbed energy of the B $|e'\rangle$ state, δ' and Ω'_c are the detuning and Rabi frequency for the strongest transition involving the $|e'\rangle$ state. The approximation is valid if $\delta' \gg \Omega'_c$.

The parameters in Eq. (13) must be chosen in such a way that the B line is not distorted. If one can choose the control field such that the detunings of all the relevant transitions are high, and the corresponding dipole matrix elements are small, then the B absorption lines

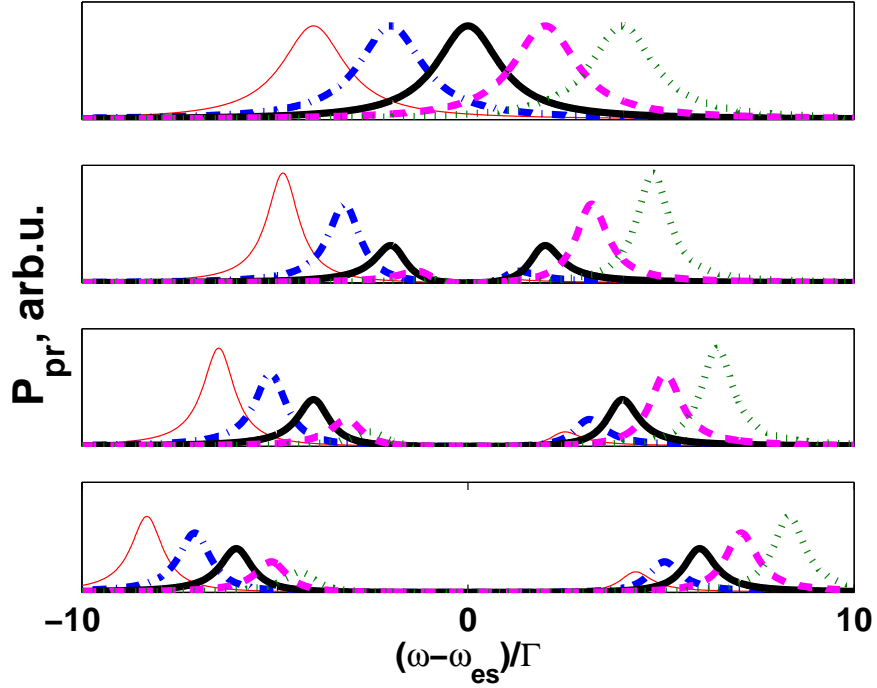


FIG. 5: (Color online). Few close lying transitions of the control field which are close to the probe transition frequency too. We demonstrate the behavior of the spectrum in several control amplitudes. (a): $\Omega_c = 0\Gamma$; (b): $\Omega_c = 2\Gamma$; (c): $\Omega_c = 4\Gamma$; (d): $\Omega_c = 6\Gamma$.

will be observed at their natural positions. Making an order-of-magnitude estimate, we see that if δ and Ω_c of the A lines satisfy the $\delta < \sim \Gamma$, and $\Omega_c \simeq \Gamma$ conditions, the method will work if we can move the A lines by about a line width. Assuming that the B Rabi frequencies are of the same order: $\Omega'_c \simeq \Gamma$ (which is rather pessimistic because the control frequency is off-resonance with respect to the B absorption), the requirement that the B line position not be moved by much means, using Eq.(13), that

$$\delta' \gg \Gamma . \quad (14)$$

The method will not work if the molecule has a dense spectrum near *both* the $|e\rangle$ and the $|s\rangle$ states, and if many of the e - s transitions are strong. In this case, due to the many AT-split e levels the A spectrum may not part away sufficiently from the spectral region of interest.

4. APPLICATIONS TO REAL MOLECULES

We now present three realistic cases where we successfully implement EIT spectroscopy.

4.1. Two isotopomers of Cl₂.

As *B* lines we choose transitions belonging to the ³⁵Cl³⁷Cl minority isotopomer. As *A* lines we choose transitions belonging to the ³⁵Cl₂ majority isotopomer. Table 1, obtained from Ref.[34], shows the frequencies of several $X^1\Sigma_g^+ - B^3\Pi_0^+$ transitions of ³⁵Cl₂ and ³⁵Cl³⁷Cl. The table shows several pairs of “intramolecular” and “intermolecular” overlapping lines whose line-widths are typical of gas-phase conditions. For example, the ³⁵Cl₂ $R_{v_2-9}^{J=59}$ transition and the ³⁵Cl³⁷Cl, $P_{v_1-9}^{J=28}$ transition strongly overlap. (Here *P* stands for a $\Delta J = -1$ transition, *R* - for a $\Delta J = 1$ transition, with the subscript denoting the vibrational quantum numbers involved in the transition. *J* designates the angular momentum of the lower state).

Since diatomic rotational energies can be approximated as

$$E_{rot} = B_v J(J + 1) + \text{const}, \quad (15)$$

the separation between neighboring rotational levels increases linearly with *J*. It therefore makes sense to consider the case of high *J* *A* lines because such lines are separated from other rotational transitions. We have thus chosen the ³⁵Cl₂ $R_{v_2-9}^{J=59}$ transition as our *A* line, with $|g\rangle$ being the ³⁵Cl₂ $X^1\Sigma_g^+(J = 59, v = 2)$ state and $|e\rangle$ being the $B^3\Pi_0^+(J = 60, v = 9)$ state. Given this *A* line, the auxiliary $|s\rangle$ state was chosen to be the ³⁵Cl₂ $X^1\Sigma_g^+(J = 59, v = 4)$ state, giving rise to transition frequency of $\omega_{e,s} = 1.3286 \cdot 10^4 \text{ cm}^{-1}$.

The control field was chosen to be detuned from the *B* lines of the ³⁵Cl³⁷Cl molecule by $\delta' = 9 \text{ cm}^{-1}$, with the control Rabi frequency being $\Omega'_c = 10^{-2} \text{ cm}^{-1}$. The *B* line shift, calculated according to Eq. (13), of 10^{-4} cm^{-1} , is negligible compared to the line width. Thus, the control field leaves the position and shape of the ³⁵Cl³⁷Cl, $P_{v_1-9}^{J=28}$ line essentially untouched, as required. We conclude that EIT spectroscopy allows us to effectively eliminate transitions of the majority ³⁵Cl₂ isotopomer which overlap with transitions associated with the ³⁵Cl³⁷Cl minority isotopomer.

4.2. Eliminating two “intramolecular” overlaps in the Chlorine molecule.

As surmised from Table 1, there is a strong overlap between the $P_{v_1-9}^{J=5}$ and $R_{v_2-9}^{J=59}$ lines in

Isotopomer	$^{35,35}\text{Cl}_2$ v_{2-9} band	$^{35,37}\text{Cl}_2$ v_{1-9} band	$^{35,35}\text{Cl}_2$ v_{1-9} band
Rotational Branch, ω_{ge} (cm^{-1})	$R_{J=59},$ $1.312 \cdot 10^4$	$P_{J=28},$ $1.312 \cdot 10^4$	$P_{J=5},$ $1.312 \cdot 10^4$
Rotational Branch ω_{ge} (cm^{-1})	—	$R_{J=32},$ $1.3122 \cdot 10^4$	$R_{J=7},$ $1.322 \cdot 10^4$
Rotational Branch, ω_{ge} (cm^{-1})	$P_{J=55},$ $1.3119 \cdot 10^4$	$R_{J=33},$ $1.3119 \cdot 10^4$	—

TABLE I: Overlapping lines in $^{35,35}\text{Cl}_2$ and $^{35,37}\text{Cl}_2$. The letters P and R refer to the rotational branches $\Delta J = \pm 1$.

line	transition	frequency, [cm^{-1}]
(a)	$P(1, 10; 22)^0 \leftarrow (0, 9; 23)^0 A$	231.14691
(b)	$Q(1, 5; 18)^0 \leftarrow (0, 4; 18)^0 E$	231.14924
(c)	$Q(1, 5; 19)^0 \leftarrow (0, 4; 19)^0 E$	231.15178
(d)	$Q(1, 5; 17)^0 \leftarrow (0, 4; 17)^0 E$	231.15353

TABLE II: Overlapping lines in CH_3OH [35].

$^{35}\text{Cl}_2$. Again we choose to eliminate (an A line) originating at a rather high J quantum number. A control field with the frequency $\omega_c = 1.3286 \cdot 10^4 \text{ cm}^{-1}$ is used to couple the $|e\rangle = B^3\Pi_0^+(v = 9, J = 59)$ state to the $|s\rangle = X^1\Sigma_g^+(v = 5, J = 59)$ state. As in the above, we first verify that the parameters we choose for the control field are such as to not affect the target (B -line) $= P_{v_{1-9}}^{J=5}$ transition. In order to guarantee this, due to vibrational anharmonicity, the detuning δ' in this case must be $\sim 20 \text{ cm}^{-1}$. With this choice of parameters we can successfully “push” away the A line to reveal the (unaltered) B line.

4.3. Eliminating “intramolecular” overlaps in Methanol.

Compared to Chlorine, the spectrum of Methanol, CH_3OH , is replete with intramolecular overlaps. Table 2 lists several nearly overlapping frequencies of rotational transitions [35, 39], where the line notation is: the first entry refers to P , Q or R rotational branch; the next entry (the (n, K, J) triad) is composed of, n , the torsional quantum number; J the total

angular momentum quantum number; and K , the projection of J on the molecular-axis quantum number. The superscript 0 implies that there are no vibrational excitations in any of the states, the transitions being purely torsional and rotational. The last entry pertains to the (A or E) point group irreducible representation of both the $|e\rangle$ and $|g\rangle$ states[39].

When substantial overlaps exist, it is not an easy matter to derive numerically the individual transition line shapes from their joint envelope[35, 39]. In contrast our EIT spectroscopy can solve this problem directly: Using EIT to eliminate one of the lines from the spectrum, and comparing the resulting spectral envelopes, one can deduce the correspondent line shape.

The rotational transitions of Methanol are found in [39]. From the list, we see that a $\omega_c = 249.291 \text{ cm}^{-1}$ control field can couple the $(1, 3, 19) |e\rangle$ state to a $(0, 4; 18) |s\rangle$ state, and thus eliminate the second transition in Table 2 from the spectrum. At the same time, the control field is off resonance for transitions from the other three excited states shown in Table 2. The detuning for the $(0, 4; 19)$ and $(0, 4; 17)$ transitions is equal to 2 cm^{-1} . Repeating the arguments given above, we see that the three remaining transitions are not influenced by a control field of moderate intensity.

5. SUMMARY AND DISCUSSION

We have introduced EIT spectroscopy and have shown that through it it is possible to resolve overlapping spectral lines. The technique uses the EIT effect to remove unwanted transitions that mask some underlying transitions of interest. We have discussed the range of applicability of the technique for both sparse and congested spectra, and have demonstrated its viability for Chlorine isotopomers and Methanol molecules.

It is interesting to relate this technique to the use of Raman spectroscopy to distinguishing between overlapping lines, as shown in Fig.6(a). We first note that the AT effect can lead to saturation of the Electronic Resonance Enhanced Coherent Anti-Stokes Raman Scattering (ERE-CARS) spectroscopy. In ERE-CARS, the pump and Stokes laser fields create a Raman coherence, driving a Raman transition from the ground state $|g\rangle$ to the excited vibrational state $|e\rangle$ of a molecule. The probe field drives a resonant transition into an excited electronic state $|s\rangle$, leading to emission of an anti-Stokes transition at frequency $\omega_{as} = E_s - E_g$. Early findings of Ref. [38] indicate that if the probe field is too strong, it may cause Autler-Townes splitting of the $|e\rangle$ state, in the way described by the equation (11), leading to saturation of

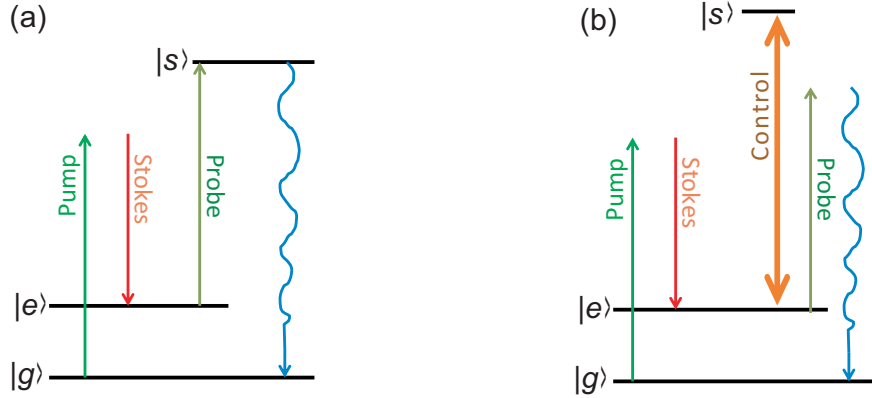


FIG. 6: (Color online). (a) ERE-CARS. The Pump and Stokes laser pulses create a Raman coherence in a molecule. The Probe drives a resonant transition into an excited electronic state $|s\rangle$, leading to emission at the frequency $\omega_{as} = E_s - E_g$. (b) EIT-assisted CARS scheme. The Pump and Stokes pulses create a Raman coherence, and the CW Probe drives emission at the anti-Stokes frequency, $\omega_{as} = \omega_e + \omega_{Probe}$. The Control field, applied simultaneously with the Probe, suppresses emission at the frequency ω_{as} .

the ERE-CARS signal.

We note that the same effect can enable distinguishing overlapping lines of different molecules. The implied scenario is similar to those discussed Section 3. The scheme is shown in Fig.6(b) for the A lines. The Pump and Stokes fields create Raman coherences in the molecule. The CW Probe, which may or may not be electronically resonant with an electronic transition, measures the resulting emission at anti-Stokes frequency of $\omega_{as} = E_e + \omega_{Probe}$. Simultaneously with the Probe, one applies a strong Control field, resonant with some electronic A transitions and non-resonant with the B transitions. Thus for the A transitions the $|e\rangle$ state is not populated, and the spectroscopic signal is suppressed. The analytical description in this case is similar to that given in Sections 2 and 3 of this paper.

Our method can also be combined with a technique proposed in Ref.[37], where it is pointed out that the population in the transition eliminated via EIT ("case A ") is trapped in the dark state $|D\rangle \simeq |g\rangle$, while the ground state $|g'\rangle$ of the B transition is depleted. A second probing, coming after the B line is measured, will find predominantly the A , rather than B , transition. Thus within a single EIT arrangement one may be able to measure, separately, each of the overlapping lines.

Further, EIT spectroscopy can be applied to measure a weak spectral line superimposed on a strong and uncontrollable background. In this case, one can make two measurements. In the first one, the line is measured on top of the background. In the second, a control field is applied to eliminate this line, and the background alone is measured. Comparison of the two spectra will yield the desired line shape, provided that the background is not strongly influenced by the control field.

Acknowledgments.

This work was supported by DTRA, NSERC, and by a Major Thematic Grant of UBC's Peter Wall Institute for Advanced Studies.

References

- [1] S. E. Harris, Phys. Today, **50**, 36 (1997).
- [2] K. -J. Boller, A. Imamoglu, and S. E. Harris, Phys. Rev. Lett., **66**, 2593 (1991).
- [3] J. Field, K. Hahn, and S. E. Harris, Phys. Rev. Lett., **67**, 3062 (1991).
- [4] M. Fleischhauer, A. Imamoglu, and J. P. Marangos, Rev. Mod. Phys., **77**, 633 (2005).
- [5] S. Autler, and C. Townes, Phys. Rev., **100**, 703 (1955).
- [6] M. Shapiro, J. Chem. Phys., **56**, 2582 (1972).
- [7] U. Fano, Phys. Rev., **124**, 1866 (1961).
- [8] G. Kurizki, M. Shapiro, and P. Brumer Phys. Rev. B, **39**, 3435 (1989).
- [9] M. Shapiro, Phys. Rev. A., **75**, 013424 (2007).
- [10] E. Arimondo and G. Orriols, Lettere Al Nuovo Cimento, Series 2, **17**, 333 (1976).
- [11] E. Arimondo, Prog. in Optics, **35**, 257 (1996).
- [12] N. Bloembergen Pure and Applied Chemistry, **55**, 1229 (1987).
- [13] R. J. H. Clark, *Advances in Non-Linear Spectroscopy (Advances in Spectroscopy* 1th edition, (John Wiley & Sons, New York, 1988).
- [14] P. Brumer and M. Shapiro, Chem. Phys. Lett., **126**, 541 (1986).
- [15] M. D. Lukin, M. Fleischhauer, A. Zibrov, H. Robinson, V. Velichansky, L. Hollberg, and M. Scully, Phys. Rev. Lett., **79**, 2959 (1997).
- [16] L. V. Hau, S. E. Harris, Z. Dutton, and C. H. Behroozi, Nature, **397**, 594 (1999).

- [17] Ch. Liu, Z. Dutton, C. H. Behroozi and L. V. Hau Nature, **409**, 490 (2001)
- [18] D. F. Phillips, A. Fleischhauer, A. Mair, R. L. Walsworth, and M. D. Lukin. Phys. Rev. Lett., **86**, 783 (2001).
- [19] A. Matsko, Y. Rostovtsev, O. Kocharovskaya, A. Zibrov, and M. Scully. Phys. Rev. A, **64**, 043809 (2001).
- [20] T. Dey and G. Agarwal. Phys. Rev. A, **67**, 033813 (2003).
- [21] M. Fleischhauer and M. D. Lukin. Phys. Rev. A, **65**, 022314 (2002).
- [22] L. M. Duan, M. D. Lukin, J. I. Cirac, and P. Zoller, Nature, **414**, 413 (2001).
- [23] P. D. D. Schwindt, S. Knappe, V. Shah, L. Hollberg, J. Kitching, L.-A. Liew, and J. Moreland, App. Phys. Lett., **85**, 6409 (2004).
- [24] C. Affolderbach, C. Andreeva, S. Cartaleva, T. Karaulanov, G. Mileti, and D. Slavov, App. Phys. B. **80**, 841 (2005).
- [25] A. Taichenachev, A. Tumaikin, and V. Yudin, Phys. Rev. A., **61**, 011802 (1999).
- [26] A. Lezama, S. Barreiro, and A. Akulshin, Phys. Rev. A., **59**, 4732 (1999).
- [27] Y. I. Heller and A. K. Popov Opt. Commun., **18**, 449 (1976).
- [28] P. E. Coleman, P. L. Knight, and K. Burnett, Opt. Commun., **42**, 171 (1982); P. L. Knight, M. A. Lauder, and B. J. Dalton, Phys. Rep., **190**, 1 (1990).
- [29] S. Cavalieri, R. Eramo, L. Fini, M. Materazzi, O. Faucher, and D. Charalambidis, Phys. Rev. A, **57**, 2915, (1998).
- [30] T. Halfmann, L. P. Yatsenko, M. Shapiro, B. W. Shore and K. Bergmann, Phys. Rev. A, **58**, R46 (1998).
- [31] C. Goren, A. Wilson-Gordon, M. Rosenbluh, and H. Friedmann, Phys. Rev. A., **69**, 063802 (2004).
- [32] E. W. Smith, M. M. Hessel, and R. E. Drullinger Phys. Rev. Lett., **33**, 1251 (1974).
- [33] C. D. Caldwell, F. Engelke, and H. Hage, Chem. Phys., **54**, 21 (1980).
- [34] J. A. Coxon and R. Shanker, J. Mol. Spectry, **69**, 109 (1978).
- [35] G. Moruzzi and H. Xu, J. Mol. Spectry, **165**, 233 (1994).
- [36] M. Shapiro and P. Brumer, *Principles of the quantum control of molecular processes* (John Wiley & Sons, New York, 2003)
- [37] A. Ch. Izmailov, Laser Physics, **18**, 855 (2008).
- [38] N. Chai, R. P. Lucht, W. D. Kulatilaka, S. Roy, and J. R. Gord, J. Chem. Phys., **133**, 084310

(2010).

[39] G. Moruzzi, F. Struma, J. C. S. Moraes *et al.*, *J. Mol. Spectry*, **153**, 511 (1992).